Effects of Nozzle Geometry on Characteristics of 3D Surface Attaching Jets

Mohammad S. Rahman[1], Baafour Nyantekyi-Kwakye[1], Mark F. Tachie[1,*]

[1]Department of Mechanical Engineering, University of Manitoba, Winnipeg, Canada
*corresponding author: mark.tachie@umanitoba.ca

Abstract An experimental study was carried out to investigate the effects of nozzle geometry on the characteristics of three-dimensional surface attaching jets. Circular, square and rectangular shapes of nozzle were used in the experiments with the same equivalent diameter of 10 mm. The aspect ratio of the rectangular jet was 3 and both of its minor and major axis orientation were tested. The experiments were conducted at a constant Reynold number of 4000. Particle image velocimetry (PIV) was used as the velocity measuring technique. The measurements were performed at the vertical symmetry plane of the jet. There was significant effect of the nozzle geometry on the reattachment point and the recirculation region of the jets. Entrainment of the ambient fluid, the centerline velocity decay and the jet spread were influenced by the shape of the nozzle exit. Effect of the free surface was noticed on the growth of the two shear layers and the mixing zone of the jets. The rectangular nozzle with minor axis orientation showed better mixing performance and larger mixing zone in the lower portion of the jet. Axis-switching of the rectangular jet was identified. The nozzle geometry as well as the presence of the free surface affected the turbulence intensities and the Reynolds shear stress distribution.
Keywords: 3D Surface jet, Turbulence features, Nozzle geometry, PIV measurement technique.

1 Introduction

Interaction between turbulent jet and free surface is a frequently encountered fluid mechanics problem in environmental and engineering applications. Examples include ocean surface and flow structure interaction, disposal of industrial and communal waste in water bodies, and turbulent wake produced by ship. A general configuration of this type of jet is shown in Fig. 1. The origin of the Cartesian coordinate system is located at the center of the nozzle exit; x and y indicate the streamwise and surface-normal direction, respectively. The streamwise and surface-normal mean velocities are denoted by U and V, respectively, and U_j indicates the maximum streamwise mean velocity along the nozzle centerline. The streamwise and surface-normal turbulence intensities and the Reynolds shear stress in x-y plane are denoted by $\langle u'^2\rangle^{0.5}$, $\langle v'^2\rangle^{0.5}$ and $-\langle u'v'\rangle$, respectively, where u' and v' are the streamwise and surface-normal fluctuating velocities, respectively. The nozzle width and the offset height of the center of the nozzle from the free surface are denoted by d and h, respectively. The jet reattaches to the free surface due to the Coanda effect. As shown in the figure, x' indicates the streamwise distance measured from the reattachment point. The overall flow field can be divided into the following three distinct regions: recirculation region (I), reattachment region (II) and surface-jet region (III). The recirculation region occurs prior to the reattachment point in the upper portion of the jet within which negative streamwise mean velocity is observed. The instantaneous reattachment point at the free surface may vary with time leading to an overlap between the recirculation and surface-jet regions. The surface-jet region starts after the reattachment of the jet to the free surface. The flow field comprises of two shear layers which are demarcated by a diving line (denoted by a dash line in Fig. 1) drawn through the y location of the local maximum streamwise mean velocity, U_m. The flow fields on the upper and lower side of this dividing line are indicated as the upper and lower shear layer, respectively. The presence of these two shear layers together with the recirculation region in the vicinity of the nozzle and free surface makes the offset jet flow relatively more complex compared to the generic free jet and wall jet.

Over the past decades, the turbulence research community has made considerable efforts to advance fundamental understanding of turbulent transport phenomena in offset jets. The effect of Reynolds number and offset height ratio on the turbulence characteristics were experimentally investigated in case of 3D circular offset jet reattaching to a solid wall [1]. The Reynolds number was varied from 5000 to 20000 while the offset height ratio was varied from 0.5 to 4.0. The experiments were carried out covering a wide range of streamwise distance ($0 < x/d \leq 120$). There was a faster decay of U_m when the Reynolds number was decreased, or when the offset height ratio was increased. The jet spread in the symmetry plane increased with an increase in offset height ratio. However, the variation of the jet spread was negligible for $h/d = 0.5$ and

1.0. No significant Reynolds number effect was found on the reattachment length, the streamwise distance of the reattachment point measured from the nozzle exit. The reattachment length increased from 1.45*d* to 6.40*d* with an increase in offset height ratio within the range mentioned above. The characteristics of 2D wall attaching offset jets [2-4] were studied in a greater detail compared to its 3D counterparts.

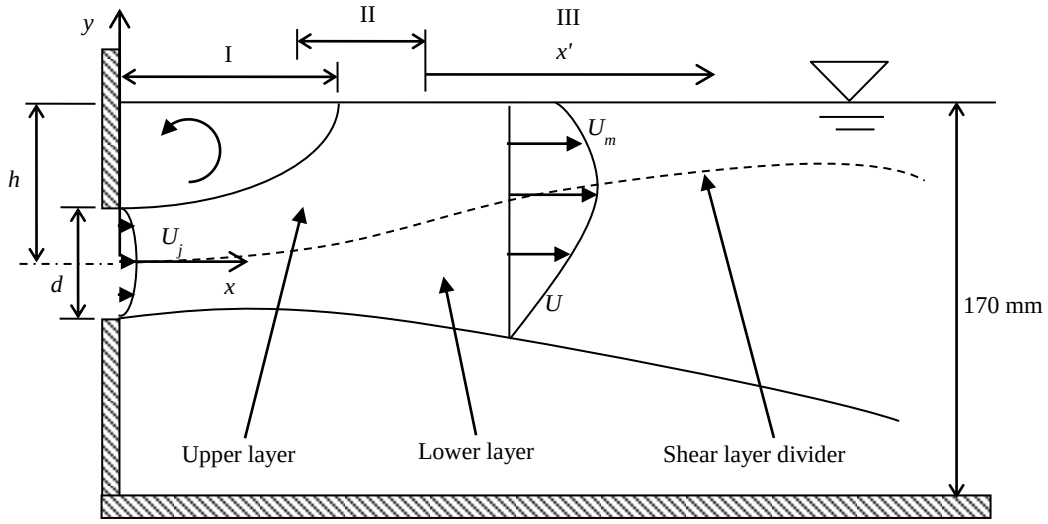

Fig. 1 Schematic of surface attaching offset jet

While wall attaching jets have been studied in detail [1-6], our present understanding of surface attaching jets is deficient. Moreover, the few surface attaching jets that were studied pertained to plane or 3D circular jets [7-9]. Tian et al. [7] studied the turbulence characteristics of surface attaching circular jet. The experiments were performed at a Reynolds number of 28000. Two offset height ratios, 5 and 30, were used in the experiment to model jet-surface interaction and reference free jet for comparison purpose. Their results showed that before the jet-surface interaction (i.e., $x/d \leq 30$), the surface jet behaved like a free jet. The location of U_m moved toward the free surface as the surface jet develops further downstream. The spread rate in the upper shear layer, i.e., near the free surface, was observed to be larger compared to the spread rate of a free jet. A reduction of the streamwise, surface-normal and lateral turbulence intensities was observed near the free surface. The effect of both the free surface and a solid wall on the characteristics of a circular jet was investigated by placing the nozzle at the middle of the free surface and the bottom of the channel using a limited depth of water [8]. Three offset height ratio of 2, 3 and 4 were tested. The results clearly showed that the velocity distribution in the vertical plane within the near field region was similar to that of free jet. Tsunoda et al. [9] found from their plane jet study that the jet reattached to its nearest boundary once the offset height ratio was limited to 7.5, 15, 22.5 and 30 from both the free surface and the solid wall. No effect of the opposite boundary on the characteristics of jet flow such as centerline velocity decay, and jet spreading was observed after the reattachment of the jet to the nearest boundary. When the offset height from both of the boundary was equal, the reattachment of the jet to any boundary was unpredictable. In that case the jet may reattach to the free surface or to the solid wall and similar reattachment length was found in both cases. Non-circular jets were also taken into consideration for the surface jet study where single point velocity measuring techniques like laser Doppler velocimetry, hot wire anemometer were used in most of the experiments [10, 11]. The mixing characteristics of the surface jet issuing from different nozzle configurations were not studied extensively so far. On the other hand, research on turbulent free jets clearly demonstrate that the mixing performance of jets produced from non-circular and sharp-edged nozzles is superior to that observed in contoured circular jets [12].

The objective of this study is to investigate the effects of sharp-edged nozzle geometry on 3D surface jet characteristics. A particle image velocimetry (PIV) was used to measure the instantaneous velocity field. The mixing characteristics and turbulent transport phenomena are investigated using the mean velocities, jet spread and higher order turbulence statistics.

2 Experimental procedures

The experiments were performed in an open water channel. The channel was made of acrylic plate for easy optical access. The length of the channel was 2500 mm and the square cross sectional area was 200 × 200 mm^2. The following three different sharp-edged nozzles were tested: circular, square and rectangular nozzle with aspect ratio of 3. The rectangular nozzle was tested orienting its minor and major axis along y which are denoted hereafter as Rect_minor and Rect_major, respectively. The equivalent diameter, d of the nozzles was kept constant as 10 mm. The free surface was at a distance of 170 mm above the bottom of the channel. The center of the nozzle was placed below the free surface to produce an offset height ratio of $h/d = 2$. All the experiments were conducted at a fixed Reynolds number, $Re = 4000$ which is based on the streamwise bulk velocity at nozzle exit, U_b and d.

A planar PIV was used for the velocity measurement in the x-y symmetry plane of the jet. Silver coated hollow glass spheres with a mean diameter of 10 μm were used as seeding particles. The specific gravity of the seeding particles was 1.4. The flow was illuminated by the Nd:YAG double-pulsed laser which has a maximum energy of 120 mJ per pulse at 532 nm wavelength, and a charge-coupled device camera was used to image the flow field. The resolution and the pixel pitch of the camera were 2048 × 2048 pixel and 7.4 μm, respectively. The camera field of view was 84.1 × 84.1 mm^2. The interrogation area size was set to 32 × 32 pixels with 50% overlap for the data processing. The measurements were obtained in three different symmetry planes within the range of $0 \leq x/d \leq 24$. In each measurement plane, 5000 images were taken and post-processed by using DynamicStudio software to obtain the mean velocities and higher order turbulence statistics.

3 Results and discussions

Mean velocity field: Contour plots of the dimensionless streamwise mean velocity (U/U_j) are presented in Fig. 2 for circular, square, Rect_minor and Rect_major jets. All the contour plots presented in this paper spanned in the streamwise direction from the nozzle exit to $x/d = 7.5$ within which the recirculation region and reattachment point were captured. All the jets reattached to the free surface because of the Coanda effect. The zero velocity contour level in the upper shear layer is used to estimate the average reattachment point at the free surface. The average reattachment point was $x/d = 6.5$, 6.3, 4.2 and 1 for the circular, square, Rect_minor and Rect_major jets, respectively. The region bounded by the zero velocity contour level and free surface indicates the recirculation region where negative streamwise mean velocity was found. From the figure, it is observed that the recirculation region near the free surface appeared prior to the reattachment point and this region was affected by the shape of the nozzle exit. Rectangular jet caused a smaller recirculation region compared to the circular and square jets. The smallest recirculation region was observed for the Rect_major as the top edge of this particular nozzle was very close to the free surface thereby causing an early reattachment of the jet to the free surface. A larger potential core, within which the maximum streamwise mean velocity occurs and the variation of this velocity is negligible, was observed in the circular and Rect_major jet than in the square and Rect_minor jets. The velocity magnitude reduced gradually as the jet propagates downstream because of the entrainment of ambient fluid which leads to the jet spreading in the y direction. From the figure, similar trend of jet spreading was observed for the circular and square nozzles. Rect_minor jet showed a faster jet spread compared to the other jets and Rect_major jet showed the lowest spreading. Detailed discussion about the jet spreading will be presented in a later paragraph where the development of jet half width is discussed.

The dimensionless surface-normal mean velocity (V/U_j) contours are presented in Fig. 3. As the jets propagate downstream, two shear layers developed, and these shear layers were divided by the zero contour level of V at the jet centerline. Each shear layer showed negative and positive V except Rect_major case. These negative and positive values of V correspond to outward jet expansion into the ambient fluid, and the entrainment of ambient fluid into the core jet. In the upper shear layer, for example, positive V represents jet expansion while negative V corresponds to entrainment of ambient fluid into the core jet. The contour level, $V = 0$ demarcated the interface between region of outward jet expansion, and entrainment of ambient fluid into the core jet. Due to the vena contracta effect, the streamlines issuing from the sharp edge nozzle tend to converge and pressure drop occurs in the upper and lower portion of the converged streamlines. This

pressure difference allows the ambient fluid to enter into the jet flow field near the nozzle. The magnitude of the positive and negative V in the lower and upper shear layer of the jet reduced with the increasing streamwise distance indicating a reduction of the entrainment from both sides of the jet along the streamwise direction. The presence of the free surface and the nozzle geometry affected the entrainment in the upper layer. Entrainment in the upper shear layer extended in the streamwise direction up to x/d = 7.4, 6.6 and 5, respectively, for circular, square and Rect_minor jets.

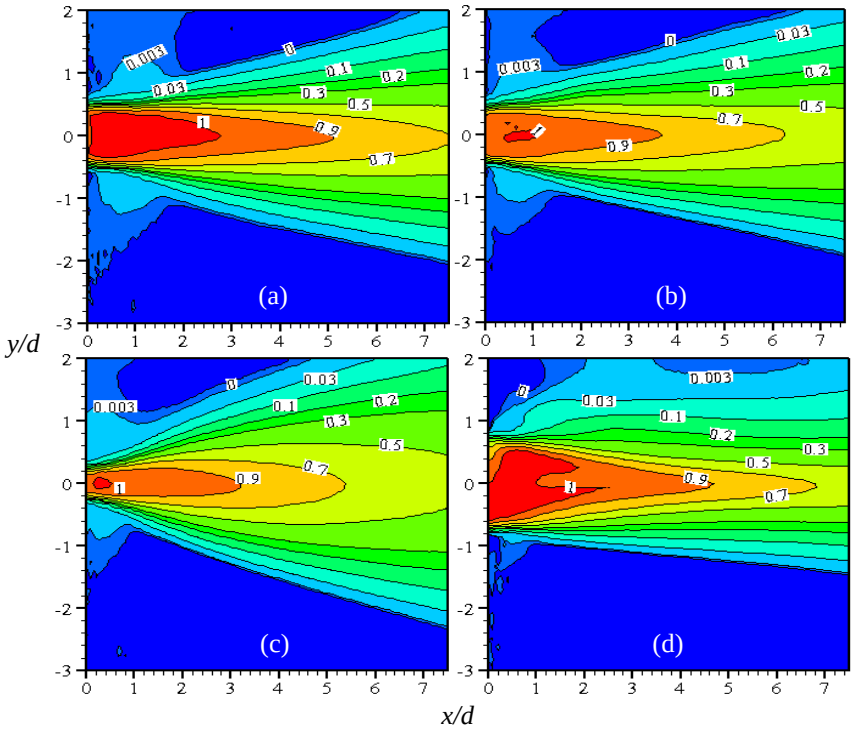

Fig. 2 Contour of U/U_j for (a) circular, (b) square, (c) Rect_minor and (d) Rect_major jets

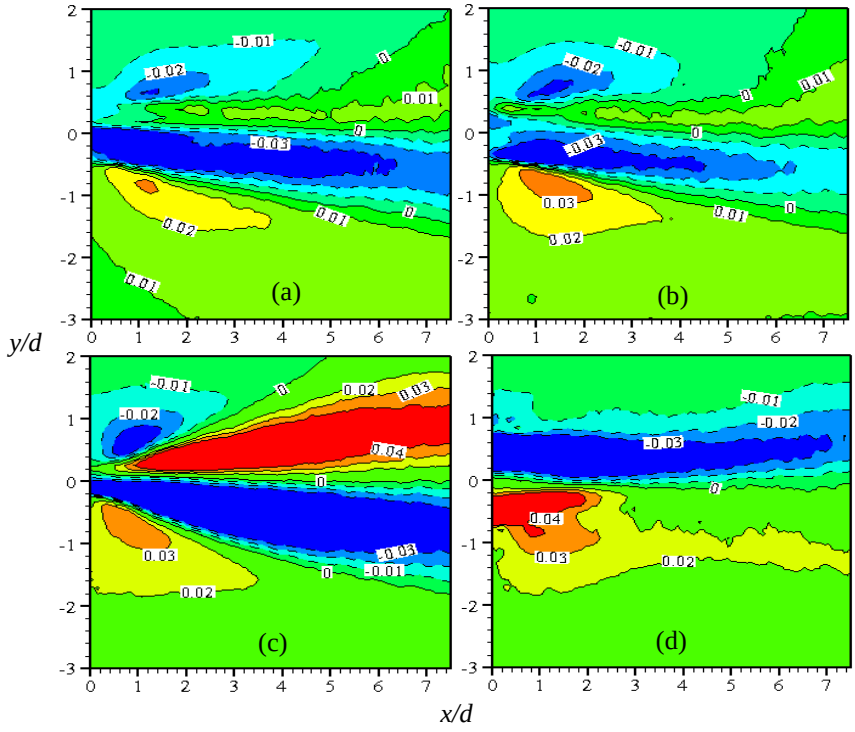

Fig. 3 Contour of V/U_j for (a) circular, (b) square, (c) Rect_minor and (d) Rect_major jets

The streamwise and surface-normal mean velocity profiles at selected streamwise locations are shown in Fig. 4. The selected locations are x/d = 0.4 (which corresponds to a location near the nozzle exit), x/d = 3 which corresponds to a location within the recirculation region (except for Rect_major case), reattachment point (RP), and x'/d = 5 and 16 which are located downstream of reattachment point. It is observed from Fig. 4 (a) that very close to the nozzle exit at x/d = 0.4, U profiles showed a top-hat shape. Circular, square and Rect_minor jets showed similar trend of U profiles as the jets develop downstream and there was similarity between these profiles and the Gaussian distribution up to the reattachment point. Similar observation was found by Tian et al. [7] in case of a circular jet. The profiles after the reattachment point, at x'/d = 5 and 16, showed that the streamwise mean velocity at the free surface increased gradually as the jet moves downward due to the free surface effect. After the reattachment point, the circular and square jets showed similar U values at the free surface, while higher U was observed in case of Rect_minor compared to the other jets.

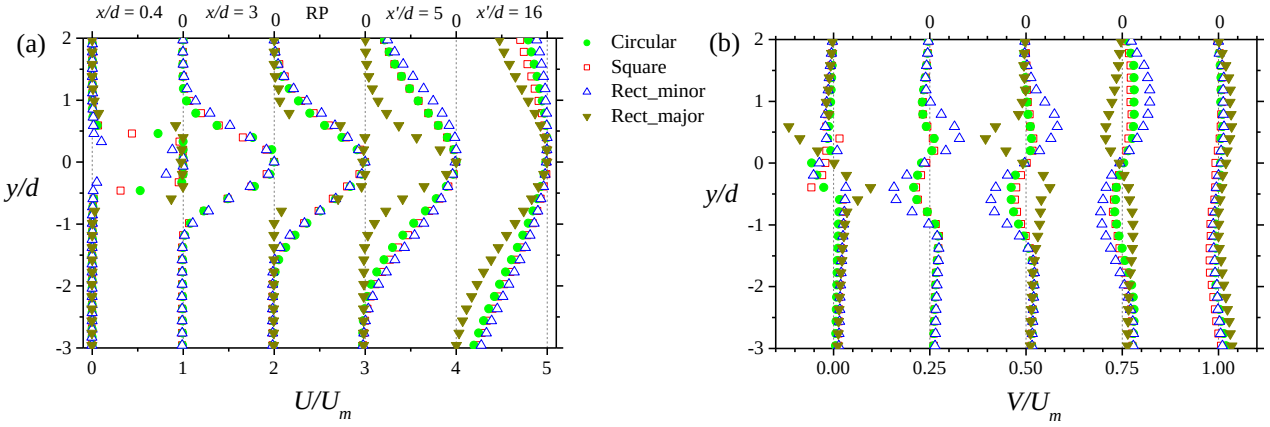

Fig. 4 Streamwise (a) and surface-normal (b) mean velocity profiles

The surface-normal mean velocity profiles in Fig. 4 (b) show higher positive and negative value of V for Rect_minor case in the upper and lower layers, respectively, compared to the circular and square jets up to the streamwise distance x'/d = 5. This indicates higher expansion of the shear layers of Rect_minor jet leading to the enhanced mixing characteristics. Higher magnitude of positive V in the lower layer was observed compared to the magnitude of negative V in the upper layer for the circular, square and Rect_minor jets. This would suggest a higher entrainment from the lower side compared to the upper side of these three types of jet. Opposite phenomenon occurred in the case of Rect_major jet, that is, the entrainment from the upper side was higher than the lower side of this jet. Low magnitude of V in both shear layers at x'/d = 16 indicated reduction of entrainment as well as the shear layer expansion at larger streamwise distance from the exit plane.

Centerline velocity decay and jet spreading: Streamwise mean velocities along the nozzle centerline are shown in Fig. 5 (a). There was a rapid increase of U near the nozzle exit because of the vena contracta effect. This is followed by a region of negligible variation of the maximum velocity which corresponds to the potential core region. Square and Rect_minor jets showed smaller potential core (up to $x/d \leq 1.2$) compared to the round and Rect_major jets (up to $x/d \leq 2.8$) as mentioned earlier. Beyond the potential core, the centerline velocity decayed rapidly due to entrainment of ambient fluid into the core jet. Square and rectangular jets showed a faster velocity decay compared to the circular jet indicating enhanced entrainment in case of non-circular jets.

The growth of jet half width, $y_{0.5}$ and $y_{-0.5}$ with streamwise distance is shown in Fig. 5 (b) where $y_{0.5}$ and $y_{-0.5}$ are the positive and negative y locations, respectively, at which $U = 0.5U_m$ occurs. The nozzle centerline is shown by the horizontal line at y/d = 0. The jet half widths of Rect_minor are smaller than for Rect_major close to the nozzle exit. These jet half widths of Rect_minor reached to that of Rect_major at x/d = 2.5 which could be considered as the location of axis-switching, which generally occurs in asymmetric jets. After x/d = 2.5, $y_{-0.5}$ spreading of Rect_minor was higher than that of Rect_major. A reduction in the $y_{-0.5}$ spreading of Rect_minor was noticed at x/d = 20, while $y_{-0.5}$ of Rect_major jet was still spreading. This would suggest that

another axis-switching may occur at a farther downstream where $y_{-0.5}$ of Rect_minor and Rect_major jets would be equal again. Axis-switching contributes to the mixing performance of asymmetric jets. The growth of $y_{0.5}$ and $y_{-0.5}$ was influenced by the free surface and showed anti-symmetric jet spreading along the nozzle centerline. The spread rate was estimated as the slope of the linear fit of the jet half width profile. The spread of $y_{0.5}$ and $y_{-0.5}$ was similar near the nozzle exit ($x/d \leq 2$) for each type of jet. After that higher spread rate of $y_{0.5}$ (0.126, 0.114, 0.181 and 0.098 for circular, square, Rect_minor and Rect_major, respectively) was observed compared to the spread rate of $y_{-0.5}$ (0.089, 0.085, 0.116 and 0.075 for circular, square, Rect_minor and Rect_major, respectively). The circular and square jets showed similar trend of the spreading while, Rect_minor jet showed a faster spread of both shear layers than the other jets.

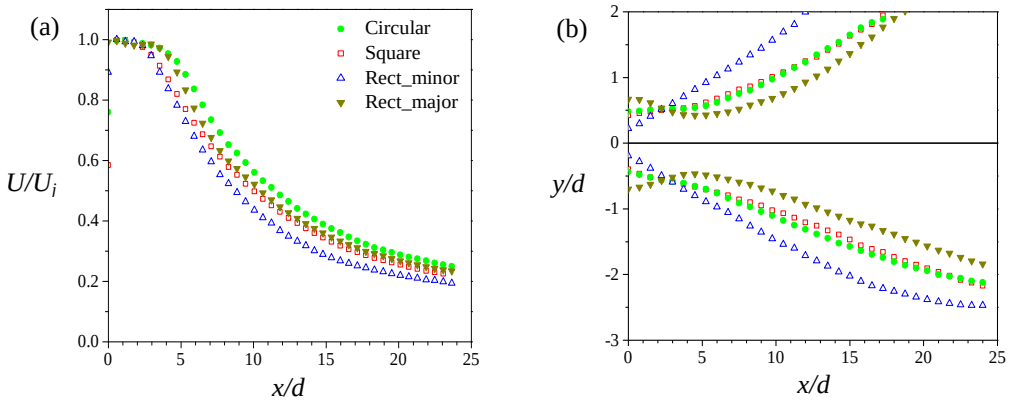

Fig. 5 Streamwise mean velocity decay along centerline (a) and jet half widths (b)

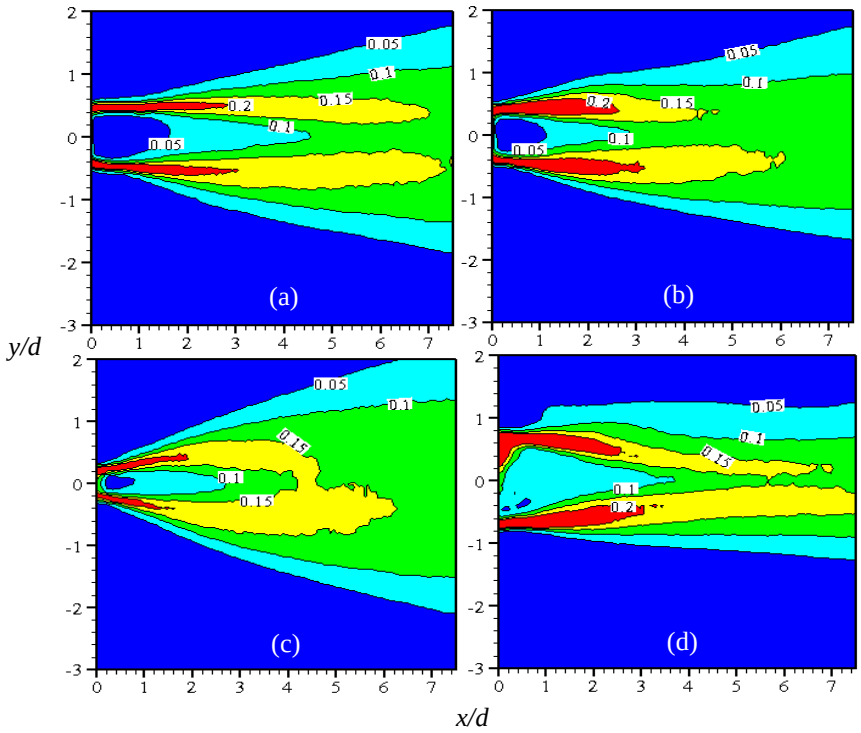

Fig. 6 Contour of $\langle u'^2 \rangle^{0.5}/U_j$ for (a) circular, (b) square, (c) Rect_minor and (d) Rect_major jets

Turbulence intensities and Reynolds shear stress distribution: Contours of streamwise turbulence intensity, $\langle u'^2 \rangle^{0.5}/U_j$ is shown in Fig. 6 for the four nozzle configurations. Close to the nozzle exit, $\langle u'^2 \rangle^{0.5}$ was negligible at the center of the nozzle and the highest $\langle u'^2 \rangle^{0.5}$ was observed at the nozzle edge. The maximum streamwise turbulence intensity occurred in the shear layers up to $x/d = 3$ for circular, square and Rect_major jets, and $x/d = 2$ for Rect_minor jet. The turbulence level reduced as the jets move towards the free surface. The spreading of $\langle u'^2 \rangle^{0.5}$ of each jet showed similar trend to its streamwise mean velocity contour. The

streamwise turbulence intensity along the centerline increased within the region $x/d \leq 6$. Subsequently, it started decreasing as the jet propagates farther downstream which is not shown in the figure. Non-circular jets experienced a faster increase of $\langle u'^2 \rangle^{0.5}$ along the centerline.

Contours of Reynolds shear stress, $-\langle u'v' \rangle / U_j^2$ in the *x*-*y* plane is shown in Fig. 7. The negative and positive distribution of $-\langle u'v' \rangle$ was observed in the upper and lower part of the nozzle, respectively due to the nature of the mean shear layers. The opposite phenomenon regarding the positive and negative $-\langle u'v' \rangle$ in two shear layers was noticed near the nozzle exit of Rect_major indicating a signature of axis-switching characteristics. As the jet reaches the free surface, the magnitude of $-\langle u'v' \rangle$ in the upper layer reduced. The circular and square jets showed similar $-\langle u'v' \rangle$ distribution along the surface-normal direction. For example, the negative and positive 0.001 contour level of $-\langle u'v' \rangle$ distribution of these two jets spanned within $y/d = \pm 1.6$ at $x/d = 7$. A wider $-\langle u'v' \rangle$ distribution along the surface-normal direction was observed in the Rect_minor jet.

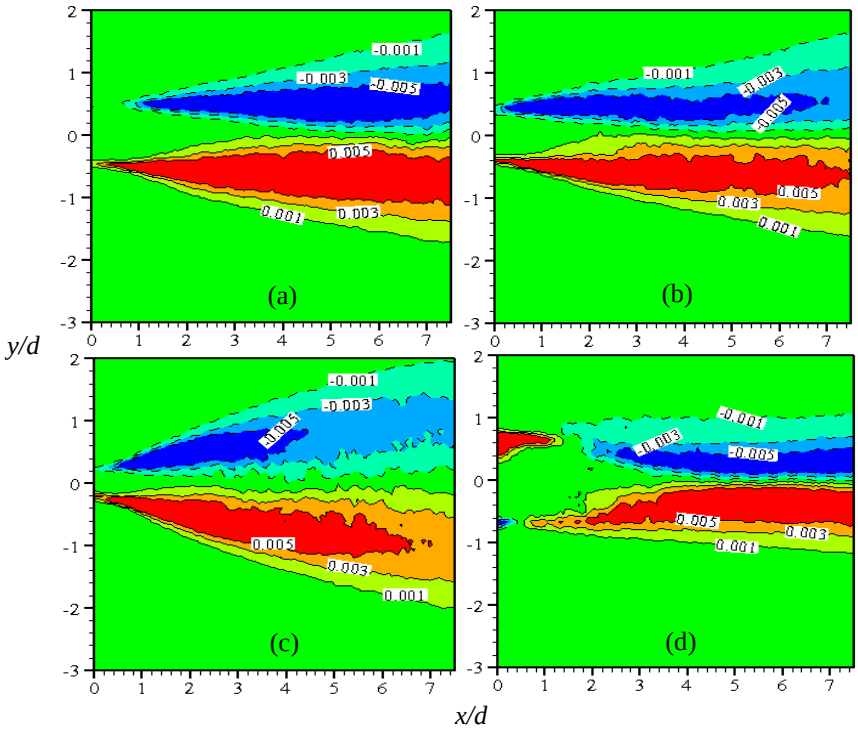

Fig. 7 Contour of $-\langle u'v' \rangle / U_j^2$ for (a) circular, (b) square, (c) Rect_minor and (d) Rect_major jets

Normalized streamwise turbulence intensity and Reynolds shear stress profiles at the same streamwise locations selected for the mean velocity profiles are presented in Fig. 8. Fig. 8 (a) showed double peak profiles of $\langle u'^2 \rangle^{0.5}$ in the region extending from the exit plane to the reattachment point. These double peaks disappeared and the maximum $\langle u'^2 \rangle^{0.5}$ occurred close to the nozzle centerline at $x'/d = 5$. The streamwise turbulence intensity at the free surface was negligible in the near-field region and gradually increased with the streamwise distance as shown at $x'/d = 5$ and 16. Similar trend of $\langle u'^2 \rangle^{0.5}$ was observed for the circular, square and Rect_minor jets at downstream locations, though the magnitude of $\langle u'^2 \rangle^{0.5}$ of Rect_minor jet was higher than the value observed in the other jet types. The profiles of surface-normal turbulence intensity, $\langle v'^2 \rangle^{0.5}$ (not shown herein) revealed a similar trend to $\langle u'^2 \rangle^{0.5}$ but are generally smaller in magnitude.

From Fig. 8 (b), negligible $-\langle u'v' \rangle$ distribution is observed near the nozzle exit at $x/d = 0.4$ and at the reattachment point in case of Rect_major jet due to its short reattachment length. As the jet evolves downstream, the effect of the free surface was observed in $-\langle u'v' \rangle$ distribution within the upper and lower shear layers leading the development of anti-symmetric profiles along nozzle centerline. Non-zero $-\langle u'v' \rangle$ was observed at the free surface at $x'/d = 5$ and 16 as there was streamwise mean velocity gradient as shown in Fig. 4 (a). The maximum values of $-\langle u'v' \rangle$ at $x/d = 3$ occurred at about $y/d = \pm 0.5$ for circular, square and Rect_minor jet. These *y* locations shifted away from the centerline as the jets evolved farther downstream. At

x/d = 3, negative and positive distribution of $-\langle u'v' \rangle$ spanned from y/d = 0 to 1 and -1, respectively for the nozzle configurations shown. These ranges of the surface-normal distance correspond to the extents of the mixing zone in the surface-normal direction [10]. Larger mixing zone in the lower portion of the jet was found compared to the upper portion with the increase of streamwise distance and Rect_minor jet showed a larger mixing zone in the lower portion of the jet compared to the other types of jet reported herein.

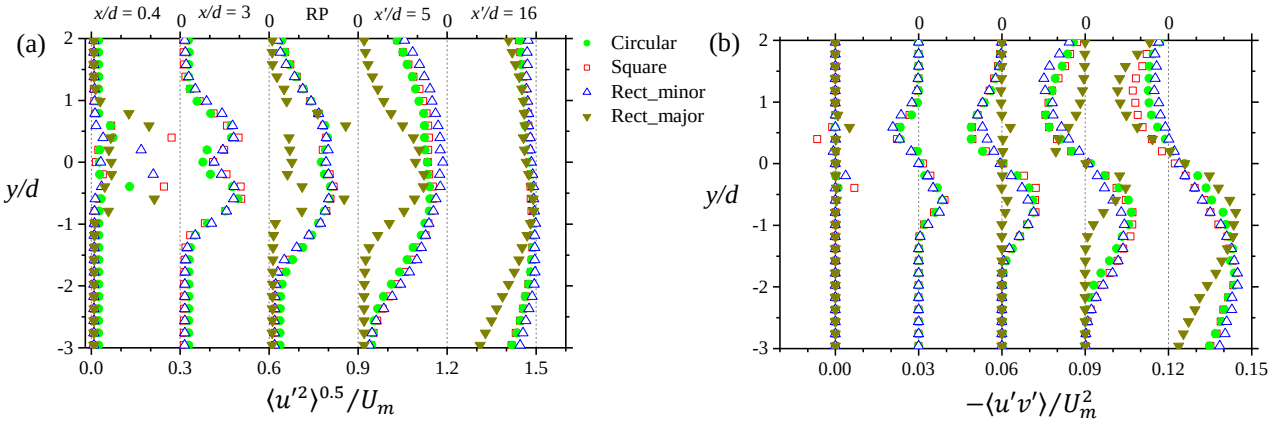

Fig. 8 Streamwise turbulence intensity (a) and Reynolds shear stress (b) profiles

4 Conclusion

Turbulence characteristics of 3D surface attaching offset jet were studied experimentally. Four different nozzle configurations: circular, square, Rect_minor and Rect_major with the same equivalent diameter were investigated. The experiments were performed at a constant Reynolds number of 4000. The mean velocity distribution revealed that the free surface and the nozzle geometry have significant impact on the reattachment point and recirculation region. The earliest reattachment occurred for the Rect_major jet, leading to a smaller recirculation region, while the circular jet had the largest reattachment length and recirculation region. Jets issuing from the rectangular nozzle showed an axis-switching phenomenon which enhances the mixing characteristics. The free surface affected the jet spread rate: a higher spread rate was observed in the upper shear layer than in the lower shear layer. The spread of both shear layers was faster in case of Rect_minor compared to the other jets.

The streamwise turbulence intensities at the center of the nozzle increased with increasing streamwise distance up to x/d = 6. There were regions of both positive and negative Reynolds shear stress due to the characteristics of mean shear layers of the offset jet. The magnitude of the Reynolds shear stress reduced as the jets propagate towards the free surface indicating the momentum transfer between the recirculation region and the upper shear layer. The presence of the free surface affected the Reynolds shear stress profiles. For example, a larger Reynolds shear stress region was observed in the lower shear layer compared to the upper layer. The results showed that Rect_minor jet provided a larger mixing zone in the lower portion of the jet.

References

[1] Agelin-Chaab M, Tachie M F (2011) Characteristics of turbulent three dimensional offset jets. *Journal of Fluids Engineering*, vol. 133, pp 1–9.

[2] Hoch J, Jiji L M (1981) Two-dimensional turbulent offset jet-boundary interaction. *Journal of Fluid Engineering*, vol. 103, pp 154–161.

[3] Nasr A, Lai J C S (1998) A turbulent plane offset jet with small offset ratio. *Experiments in Fluids*, vol. 24, pp 47-57.

[4] Pelfrey J R R, Liburdy J A (1986) Mean flow characteristics of a turbulent offset jet. *Transactions of the ASME*, vol. 108, pp 82-88.

[5] Agelin-Chaab M, Tachie M F (2011) Characteristics and structure of turbulent 3D offset jets. *International Journal of Heat and Fluid Flow*, vol. 32, pp 608–620.

[6] Nyantekyi-Kwakye B, Clark S, Tachie M F, Malenchak J, Muluye G (2014) Flow characteristics within the recirculation region of 3D turbulent offset jet. *Journal of Hydraulic Research*, pp. 1-13. doi: 10.1080/00221686.2014.950612.

[7] Tian J, Roussinova V, Balachandar R (2012) Characteristics of a jet in the vicinity of a free surface. *Journal of Fluids Engineering*, vol. 134, pp 1-12.

[8] Rainford J P, Khan A A (2009) Investigation of circular jets in shallow water. *Journal of Hydraulic Research*, vol 47: 5, pp 611–618. doi: 10.3826/jhr.2009.3474.

[9] Tsunoda H, Shimizu Y, Kashiwagi T (2006). Plane offset jet discharged into water of finite depth. *JSME International Journal*, vol. 49, pp 1111-1117.

[10] Sankar G, Balachandar R, Carriveau R (2009) Characteristics of a three-dimensional square jet in the vicinity of a free surface. *Journal of Hydraulic Engineering*, vol. 135:11, pp 989-994. doi: 10.1061/(ASCE)0733-9429(2009)135:11(989).

[11] Wolf D H, Incropera F P, Viskanta R (1995) Measurement of the turbulent flow field in a free-surface jet of water. *Experiments in Fluids*, vol. 18, pp 397-408.

[12] Manivannan P, Sridhar B T N (2013) Characteristic study of non-circular incompressible free jet. *Thermal Science*, vol. 17: 3, pp 787-800.